A Disturbance-Inventory Framework for Flexible and Reliable Landscape Monitoring

J. Linke, G.J. McDermid, D.N. Laskin, A.J. McLane, A. Pape, J. Cranston, M. Hall-Beyer, and S.E. Franklin

Abstract

Remote sensing plays a key role in landscape monitoring, but our handling of these data in a multi-temporal time series is not yet fully developed. Of particular concern is the presence of spatial and thematic errors in independently created maps that distort measures of landscape pattern and constrain the reliability of change analysis. In addition, there is a need to incorporate continuous attributes of cover gradients for flexible map representations that support a variety of applications. In this paper, we present a framework for generating temporally and categorically dynamic land-cover maps that provide such a reliable and adaptable foundation. The centerpiece is a spatio-temporal disturbance-inventory database, created through semi-automated change detection and conditioned with boundary-matching procedures, which can be used to backdate and update both continuous and categorical reference maps. We demonstrate our approach using multi-annual Landsat imagery from a forested region in west-central Alberta, Canada, between the years 1998 and 2005.

Introduction

Over the past three decades, landscape monitoring has emerged as a major focus for geospatial research, particularly in forest ecosystems (Coppin and Bauer, 1996; Franklin, 2001; Rogan and Chen, 2004), where human activities are the source of much contemporary change (Houghton, 1994; Riitters *et al.*, 2002). In this regard, the multi-temporal analysis of remote sensing imagery has been used to assess the impact of landscape change on carbon cycling (Houghton *et al.*, 2001; Conard *et al.*, 2002; Song *et al.*, 2007), the conservation of protected areas (Vester *et al.* 2007; Huang *et al.*, 2007; Forrest *et al.*, 2008), biodiversity (Hansen *et al.*, 2001; Boentje and Blinnikov, 2007; Sader and Legaard, 2008), and wildlife habitat (Pearson *et al.*, 1999; Reyes *et al.*, 2000; Berland *et al.*, 2008). While many approaches to change detection and analysis exist (Lu *et al.*, 2004; Radke *et al.*, 2005), *post-classification analysis* is the most commonly applied in this context. The strategy involves the analysis of changes based on a series of two or more independently classified maps, where each map reflects the investigated landscape at a different instance in time (e.g., Skole and Tucker, 1993; Kozak *et al.*, 2007; Gamanya *et al.*, 2009).

A serious concern in post-classification analysis is the presence of *spurious change* arising from classification errors and spatial inconsistencies in independently generated map products (Shao and Wu, 2008; Linke *et al.*, 2009). These problems have been shown to cause significant errors, particularly in the quantification of land-cover pattern (e.g., Brown *et al.*, 2000; Langford *et al.*, 2006). In response to these issues, researchers have suggested several remediation techniques designed to improve the reliability of remote sensing-based map products for landscape monitoring, such as (a) guidelines regarding spatial resolution, data processing, accuracy levels, seasonality, and minimum mapping unit (Shao and Wu, 2008), and (b) Bayesian-based statistical corrections to post-classification change-area estimates (Van Oort, 2005). However, while these strategies may serve to reduce the occurrence of spurious changes due to classification differences, they will not eliminate them.

An alternative approach to multi-temporal mapping that can reduce the issue of spurious change is to avoid the independent classification of images from different time periods, and focus instead on updating (projecting forward in time) and backdating (projecting backward in time) an existing map product through bi-temporal change detection (Coppin *et al.*, 2004). A major benefit of this approach is that by limiting the scope of re-classification to include only those areas where change has been detected, one can drastically reduce the introduction of new errors. This is akin to the visual interpretation approach to updating an existing land-cover map through manual editing of a vector-based map. After editing, the updated and original vector layers can be compared, and the associated changes stored in a spatio-temporal database. Feranec *et al.* (2000 and 2007) used this approach to update and backdate baseline maps, allowing features to appear, disappear, change thematically, or increase/decrease in size. However, these manual approaches are extremely labor-intensive, and the separation of technical inconsistencies from real change on the ground is challenging (Jansen *et al.*, 2008; Jansen *et al.*, 2006; Käyhkö and Skånes, 2006). It would be highly desirable to incorporate automated approaches to change detection and multi-temporal land-cover mapping strategies within the structured framework of a spatio-temporal database.

J. Linke, G.J. McDermid, D.N. Laskin, A.J. McLane, and M. Hall-Beyer are with the Foothills Facility for Remote Sensing and GIScience, Department of Geography, University of Calgary, 2500 University Dr. NW, Calgary A.B., T2N 1J6, Canada (jlinke@ucalgary.ca).

A. Pape and S.E. Franklin are with the Environmental Remote Sensing Laboratory, Department of Geography, University of Saskatoon, Saskatoon, S.K., S7N 4P3, Canada.

J. Cranston is with Arctos Ecological Services, 571 Mountain St., Hinton, A.B., T7V 1H9, Canada.

Photogrammetric Engineering & Remote Sensing
Vol. 75, No. 8, August 2009, pp. 981–995.

0099-1112/09/7508–0981/$3.00/0

Despite significant methodological advancements in the automatic *detection* of change features with remote sensing (e.g., Desclée *et al.*, 2006; Blaschke, 2005), little emphasis has been placed on the *integration* of these features into existing map products. The operation is problematic, due to potential variation in spatial resolution, registration errors, illumination conditions, and object segmentation results between the two time periods (Yuan and Elvidge, 1998; McDermid *et al.*, 2008). Issues arise when the boundaries of disturbance features delineated using change analysis do not precisely match with shared boundaries in the existing reference map. Under these conditions, overlay operations applied in the updating or backdating procedure will generate small artifacts of spurious change, which can limit the quality of the finished product, and cause serious problems with subsequent interpretation (McDermid *et al.*, 2008; Linke *et al.*, 2009). These spatial errors are well known in the GIS literature as *slivers*, and constitute one of the biggest challenges associated with spatial overlay operations (e.g., Goodchild, 1978; Chrisman, 1989; Mas, 2005), though they have received scant attention in the remote sensing community.

Additional concerns surrounding landscape monitoring revolve around our understanding of how to best represent land-cover and vegetation in a forested environment. Unfortunately, many remote sensing products can be criticized for presenting an overly-simplistic depiction of the natural landscape; a situation based at least in part on historical limitations of satellite data and the ubiquitous use of classification as an information-extraction technique (McDermid *et al.*, 2005). However, forested ecosystems are comprised of a complex interplay of continuous gradients of variation (Betts *et al.*, 2007; McGarigal and Cushman, 2005; Wiens, 1994) and are not well characterized by a single *catch-all* map product: particularly a categorical one produced exclusively by classification. Recent discussions on the limitations of classification in multi-disciplinary work (McDermid *et al.*, 2005) have pointed out the problems with low-level (nominal or ordinal) information layers, and the difficulty in adjusting thematic class boundaries in the finished maps. These practical challenges can hamper our efforts to understand forest dynamics, and likely contribute to the criticism of remote sensing that appears occasionally in the literature (e.g., Plummer, 2000; Thogmartin *et al.*, 2004; Gottschalk and Huettmann, 2006). McDermid *et al.* (2005) argued for the use of multi-layer information databases over single catch-all map products, and an increased emphasis on continuous, ratio-level end products that retain their flexibility. The strategy has been recently employed in the creation of single-date maps of spatially continuous representations of percent forest species composition and crown closure in layers that can be merged with basic land-cover information in a GIS to produce composite maps with many possible legends (McDermid, 2005). We believe that these emerging approaches have an important role to play in reliable and adaptable landscape monitoring.

The recent release of the Landsat archive (Woodcock *et al.*, 2008) represents a tremendous opportunity to pursue research programs that monitor the long-term temporal dynamics of land-cover using this exceptional data set (e.g., Homer *et al.*, 2007; Huang *et al.*, 2007; Kuemmerle *et al.*, 2007). However, in order to undertake such studies effectively, we require better strategies for creating reliable, spatially consistent time series of map products, that are free of spurious changes, and ideally, well-suited for supporting multiple applications. The goal of the research reported in this paper was to develop a framework for performing flexible and reliable landscape monitoring with remote sensing, using a semi-automated backdating and updating approach designed to generate temporally and categorically dynamic land-cover maps. In this manuscript, we provide a detailed description of the proposed methodological approach for creating time series of both discrete and continuous land-cover maps, presented within the context of the overall conceptual framework. We then demonstrate the effectiveness of the approach through a practical eight-year monitoring application over a large, multi-use study area in west-central Alberta, Canada using Landsat imagery.

Proposed Methodological Approach: Spatially Consistent Backdating and Updating with a Disturbance Inventory

Under ideal conditions, an existing thematic map product can be backdated and updated to produce a spatially consistent time series, representing the basic succession of ground features over time (Figure 1). The existing map at time T_0 constitutes the reference for all *dynamic features* that are to appear, disappear, and/or change over the observed time frame. Two types of dynamic features exist: (a) those that originate during the overall time interval monitored ($T_{-n} - T_{+n}$) (e.g., the small cutblock in the northern part of Figure 1 that originates between T_0 and T_{+1}), and (b) those that pre-date the beginning of the time series ($T_{\leq -n}$), but change thematically over the course of the monitoring period (e.g., the cutblock in the southeastern part of Figure 1 that changes from shrub land cover in T_{-2} to forest in T_{+2}). The remaining features, which do not change over the observed time frame, constitute s*tatic features* of the reference map (e.g., the road section in the eastern part of Figure 1 that does not change between T_{-2} and T_{+2}).

Backdating of dynamic features can follow one of four possible scenarios: (a) *feature insertion*, in which an entity is inserted into the reference map to reveal a feature that was present at the backdated stage but has disappeared from the reference map by blending into its surroundings (e.g., the cutblock inserted into the south-central portion of Figure 1 with shrub land cover in years T_{-1} and T_{-2}), (b) *feature regression*, in which an entity in the reference map changes thematically to a previous successional stage in the backdated map (e.g., the central cutblock in Figure 1 that regresses from a herbaceous land-cover in the reference map to a barren land-cover in year T_{-1}), (c) *feature persistence*, in which an entity in the reference map persists and undergoes no thematic change in the backdated map (e.g., the south-eastern cutblock in Figure 1 that persists unchanged from the reference condition in the years T_{-1} and T_{-2}), or (d) *feature removal*, in which an entity from the reference map is removed in the backdated map to reveal an earlier feature (e.g., the southern wellsite in Figure 1 with barren land cover in T_0 which is removed in T_{-2} to reveal a partially forest and partially shrub land-cover area). Similarly, updated dynamic features can follow four possible scenarios: (a) *feature insertion*, in which an entity is detected in an updated map that did not appear in the reference year (e.g., the northern cutblock in Figure 1 with barren land cover in T_{+1} in an area that appears forested in T_0), (b) *feature succession*, in which an entity existing in, or inserted into the reference map, changes thematically to a later successional stage (e.g., the northern cutblock in Figure 1 with barren land cover in T_{+1} and herbaceous land cover in year T_{+2}), (c) *feature persistence*, in which an entity in the reference map persists and undergoes no thematic change in the updated map (e.g., the road and wellsite in Figure 1 with barren land cover in years T_0 through T_{+2}), and (d) *feature removal*, in which an entity in the reference map blends into its surroundings in the updated map (e.g., the south-eastern cutblock in Figure 1 with shrub cover in T_0 developing to forest in T_{+2}).

Guided by the concepts described above, a methodological approach for generating spatially consistent backdated and

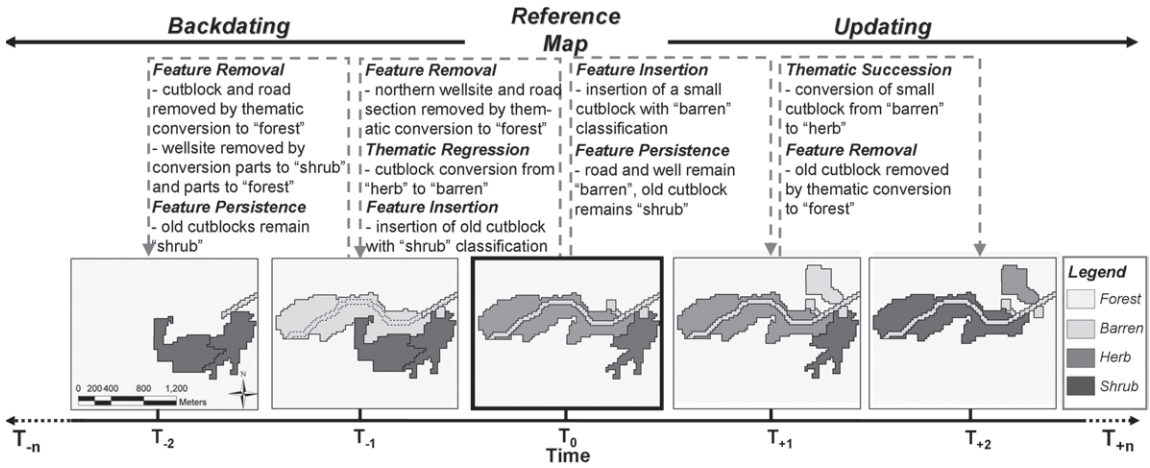

Figure 1. An ideal representation of a spatially consistent time series created by backdating and updating an existing thematic land-cover map, wherein features persist, are removed, or inserted, and display their thematic attribute according to their successional stage of development.

updated map products can be proposed. Changes in the time series described can be achieved through the identification of dynamic features as *spatially segregated entities* and their integration into the reference map with temporally relevant land-cover labels, using an *overlay order* that corresponds logically to the sequence of their appearance on the ground. The best way to implement this strategy is through the creation of a database that stores spatially referenced dynamic entities and their corresponding thematic attributes. Using the previous time series displayed in Figure 1 as an example, we refer to the dynamic entities as *disturbance features*, since the actual agents of change are disturbance based. The database of disturbance features is referred to as the *disturbance inventory* (Figure 2). *Backdated* map products can be created from existing reference maps using a disturbance inventory (e.g., the backdated land-cover map labeled T_{-2} in Figure 2) by overlaying the existing reference map with a *backdate layer* that is comprised of the relevant features from the disturbance inventory assigned with the correct thematic labels. Similarly, *updated* map products can be created from an existing

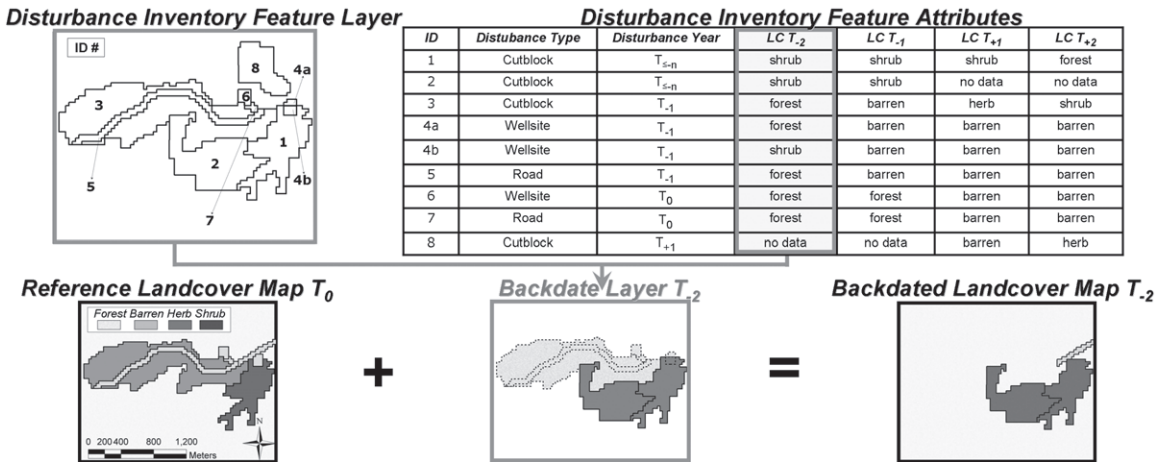

Figure 2. The proposed methodological approach for generating a spatially consistent time series of thematic land-cover through the use a disturbance inventory. Dynamic features over the time series period are detected as spatially segregated objects, classified according to the disturbance type and year of origin (i.e., disturbance year), and assigned land-cover (LC) attributes for each year of the time series. Disturbance features are organized into a database, which is subsequently used for creating backdating and updating layers to be overlaid on the original reference map to create backdated and updated land cover maps. Please note that features IDs 2 and 8 are examples of *feature insertion*. For insertions during backdating, no land-cover-label is assigned after the reference year (n/a for ID2 in LC $T_{>0}$). For insertions during updating, no land-cover label is assigned before the reference year (n/a for ID8 in LC $T_{<0}$).

reference map (e.g., the updated land-cover map at T_{+2} in Figure 2) by overlaying an *update layer* consisting of all the relevant features from the disturbance inventory labeled with their corresponding land-cover attributes.

Before the disturbance-inventory approach to backdating and updating can be applied effectively, it is crucial to consider the quality assurance criteria that must be employed. The quality of map products generated by updating/backdating strategies is a function of two basic factors: (a) the accuracy at which change features can be detected and classified, and (b) the suitability of these features for integration into the original reference map (McDermid *et al.* 2008). Regarding the first factor, if disturbance features are *not detected* and excluded from the disturbance inventory (i.e., error of omission), or if some static features are *erroneously detected* and included in the disturbance inventory (i.e., error of commission), the final multi-temporal temporal map sequence will under- or over-estimate areas of change. Similarly, if disturbance features are *erroneously classified* (e.g., a small cutblock confused with a large wellsite), the multi-temporal map sequence may exhibit *thematic errors*. Adherence to efficient change-detection protocols (e.g., Han *et al.*, 2007), robust algorithms (Sundaresan *et al.*, 2007; Walter *et al.*, 2004), and the specification of the minimum size for disturbance features can largely fulfill the needs surrounding accurate change detection.

The second factor, surrounding the seamless integration of detected disturbance features into the reference map, constitutes a methodological challenge that has rarely been described in the remote sensing literature. Unfortunately, it is virtually impossible to delineate the boundaries of disturbance features in a manner that coincides precisely with existing entities in the reference map (McDermid *et al.*, 2008; Linke *et al.*, 2009) under operational conditions. Two basic forms of spurious delineation mismatches can occur: (a) an *overshoot*, wherein the boundary of the disturbance feature extends slightly past the boundary of either a coinciding feature (Figure 3 Part A), or an adjacent feature (Figure 3 Part B) appearing in either the reference map or the disturbance inventory, and (b) an *undershoot*, wherein the boundary of the disturbance feature falls slightly short of either a coinciding feature (Figure 3 Part A), or an adjacent feature (Figure 3 Part B) existing in the reference map, or disturbance inventory. It is important to note that the specification of *overshoots* and *undershoots* in operational terms requires the definition of a minimum mapping width: the maximum allowable deviance below which mismatches are deemed spurious. Mismatches *equal to* or *larger* than the minimum mapping width are assumed to represent real changes on the ground.

Of special concern are artifacts in the backdated and updated maps that arise from boundary undershoots in disturbance feature. These errors manifest themselves in form of *sliver objects* (Figure 3 Part A), or *spurious gaps* (Figure 3 Part B) when the disturbance feature is overlaid onto the reference map. These slivers and gaps impact the visual appearance of the finished product, and can seriously distort interpretations about the direction and magnitude of multi-temporal changes in landscape pattern (Linke *et al.*, 2008). The *spurious overlaps* arising from boundary overshoots create less-conspicuous artifacts, but still contribute to inconsistent changes related to the size and shape of mapped features over the course of the monitoring horizon. A feature may appear *stretched* when a reference-map feature is overlaid with a coinciding disturbance feature with overshot boundaries (Figure 3 Part A). A feature may also appear *encroached* when an adjacent disturbance feature with overshot boundaries is overlaid (Figure 3 Part B). In order to suppress any of these spatial errors, disturbance features processing must adhere the following three boundary-matching principles: (a) the boundaries of the original reference map features should be treated as correct and must be adhered to (McDermid *et al.*, 2008), (b) the precedence among disturbance features must be established so that the order of overlay operations can be determined, and (c) a minimum mapping width must be set to delimit spurious delineation mismatches. If these principles are implemented, then precisely aligned disturbance boundaries can be generated through processing algorithms that merge spurious gaps and slivers to the adjacent disturbance feature (Linke *et al.*, 2009), and trim spurious boundary overshoots.

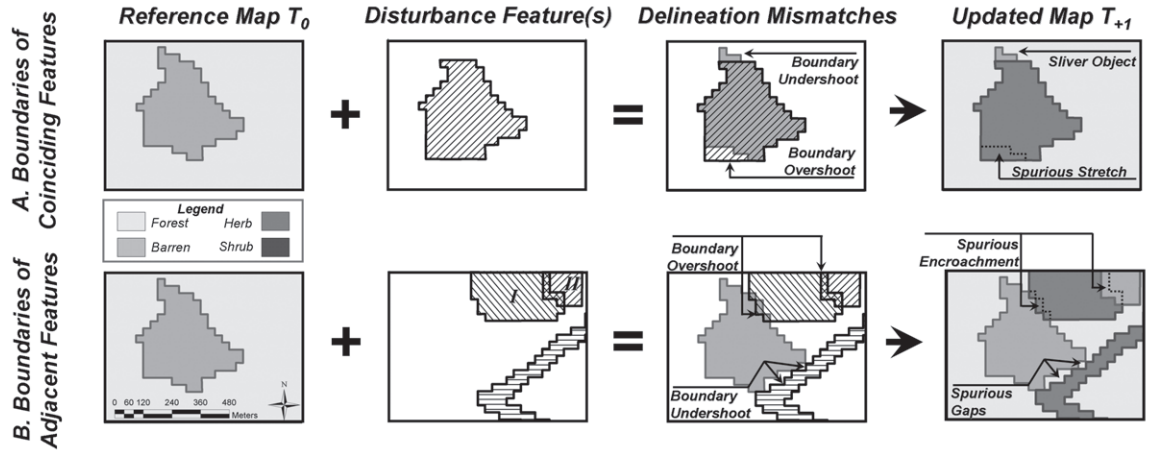

Figure 3. A demonstration of spurious boundary delineation mismatches and associated artifacts in an example map update created by the overlay of mismatched disturbance features into the reference map. The boundaries of disturbance features slightly overshoot and undershoot the boundaries of (Part A) coinciding features in the reference map, and (Part B) adjacent features in either the reference map or other disturbance features, leading to the creation of slivers, spurious gaps, spurious feature expansions, and encroachments.

The disturbance-inventory approach we propose relies therefore on two criteria: (a) disturbance features must be accurately detected, delineated, and classified into a disturbance inventory as spatially segregated disturbance features, and (b) these disturbance features must be integrated seamlessly into the reference map through the use of boundary-matching conditions and strict spatial-overlay order. It is important to note that the general application of this backdating and updating approach is not limited to the generation of categorical land-cover maps. Continuous maps of land-cover attributes, such as those representing forest crown closure (e.g., percent of canopy cover) or tree-species composition (e.g., percent relative abundance), can be handled by using the disturbance inventory as a means of identifying the areas over which the continuous reference map must be backdated or updated with new continuous-attribute values, which can be derived from the temporally relevant imagery. The strategy for accomplishing the backdating of a continuous reference map (e.g., the percent crown-closure layer represented in Figure 4) relies on the selection of all features in the disturbance inventory that originate prior to the reference year ($T_{<0}$), over which area a continuous mask can be created and integrated into the reference map. The resulting backdated mask erases any disturbance features that were originally visible in the reference map at year T_0, thereby simulating the conditions occurring earlier in the time series (T_{-n}). For each successive year, masked areas are lifted, exposing the disturbance features in their proper sequence. Updating a continuous map may be accomplished in the same manner, by replacing the values of the continuous reference map according to the timing of any post-reference year disturbance feature (Figure 4).

A Disturbance-Inventory Framework for Generating Temporally and Categorically Dynamic Land-cover Maps

A diagram explaining the conceptual framework for generating temporally and categorically dynamic land-cover maps through the backdating and updating of discrete and continuous reference maps is shown in Figure 5. The centerpiece of the framework is the spatio-temporal disturbance inventory, which contains the disturbance features and their associated attributes. In our approach, the disturbance inventory can be created using either automated or manual methods of change detection using remote sensing imagery covering the time interval *n*. Once accurately detected and classified, these features must be conditioned with boundary-matching procedures and labeled with land-cover attributes appropriate to the individual application. The disturbance inventory is employed in the generation of a spatially consistent time series of map products, derived from reference maps characterizing conditions at time T_0. The results can be described as *temporally dynamic* across the time period of interest ($T_{-n} - T_{+n}$). The framework handles either high-level (interval, ratio) or low-level (nominal, ordinal) attributes in discrete (vector) or continuous (raster) environments, depending on available data and the needs of the analyst. In the sample application below, we present a blended approach which handles map products of both types, thereby enabling the creation of *categorically dynamic* output maps whose number and types of land-cover categories are flexible, and can be generated easily through integrative post-processing routines.

Methods

Study Area and Existing Map Layers

The study area for this research was located in the west-central portion of Alberta, Canada, along the eastern slope of the Rocky Mountains (Figure 6). The 40,000 km^2 area encompasses a diverse forested landscape, and includes portions of Jasper National Park and adjacent multi-use public lands. The region is subject to a wide variety of human and natural disturbance processes, including forestry, oil and gas development, mining, road construction, forest fires, and insect defoliation: a fast-changing environment that challenges our capacity to characterize spatial change.

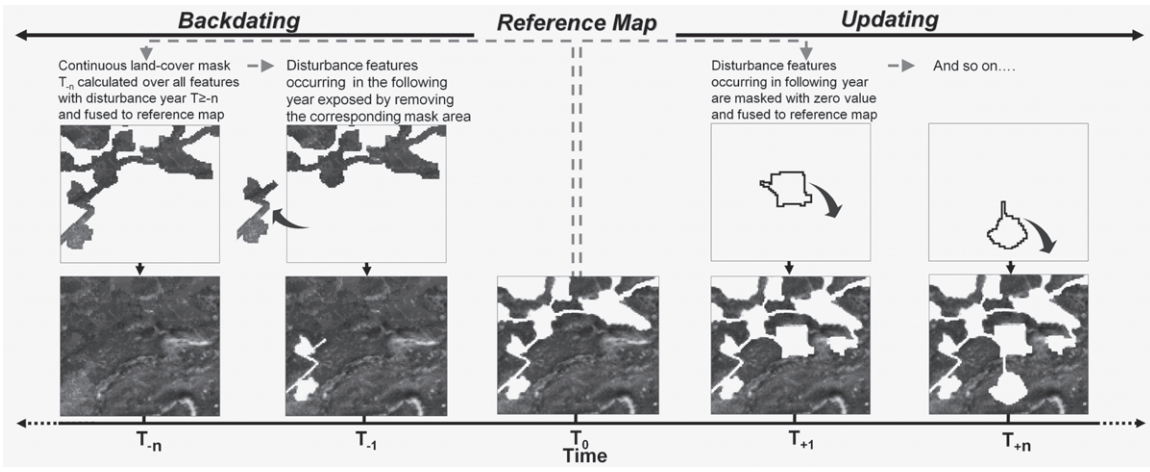

Figure 4. An example application of the principle of backdating and updating a continuous map of forest-cover attributes (percent crown closure, in this case) with a disturbance-inventory. Zero values are in white. Disturbed areas in the reference year (T_0) are identified by the disturbance inventory, and are replaced with crown closure values derived from imagery at the beginning of the time series (T_{-n}) in backdated maps. In this case, the disturbed areas originating after the reference year are inserted with values of zero for crown closure, since this area is no longer considered forested.

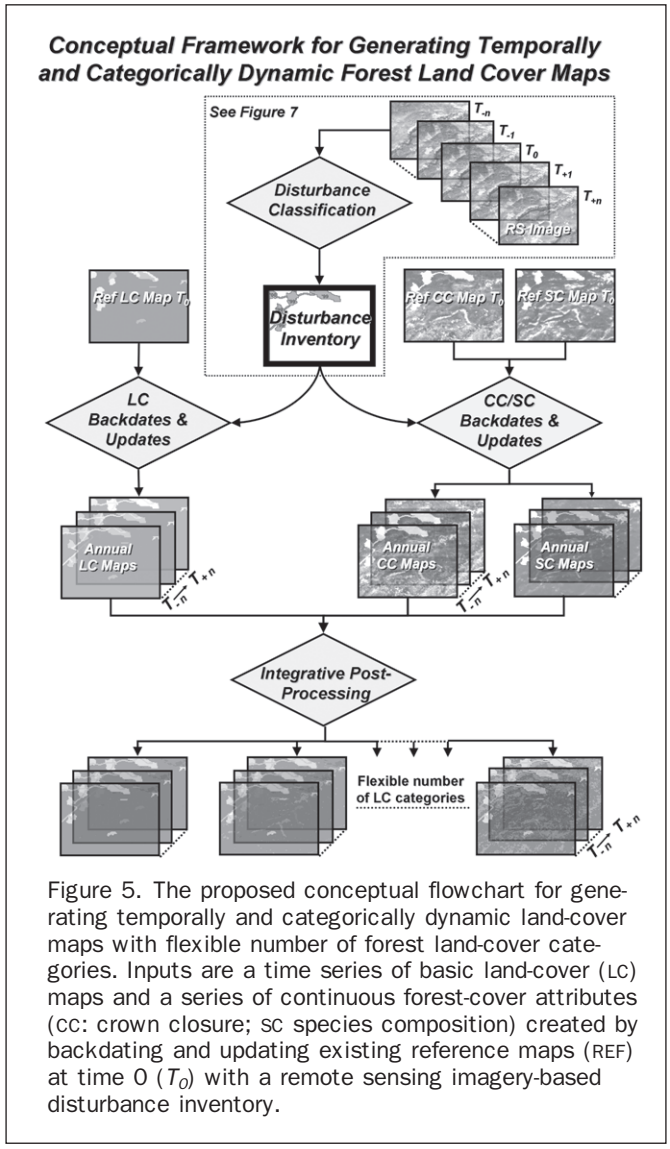

Figure 5. The proposed conceptual flowchart for generating temporally and categorically dynamic land-cover maps with flexible number of forest land-cover categories. Inputs are a time series of basic land-cover (LC) maps and a series of continuous forest-cover attributes (CC: crown closure; SC species composition) created by backdating and updating existing reference maps (REF) at time 0 (T_0) with a remote sensing imagery-based disturbance inventory.

The study area is part of the Foothills Research Institute Grizzly Bear Research Program's (FRIGBRP's) region of interest, and the work reported here represents a key element of the landscape mapping and monitoring activities taking place within that project. The FRIGBRP is a collaborative, multi-agency initiative whose main goal is the development of knowledge and planning tools designed to ensure the long-term conservation of grizzly bears in Alberta, and has been conducting work in the area since 1998 (Stenhouse and Graham, 2007). Part of these activities include the mapping and monitoring of vegetation and land-cover in support research on grizzly bear habitat selection, population, and health (Nielsen *et al.*, 2002; Nielsen *et al.*, 2004; Linke *et al.*, 2005). McDermid (2005) described the development of a three-part base map designed to provide a categorically dynamic representation of land-cover and forest structure. Existing map layers in the area include an object-based land-cover map (ten classes; 91.8 percent accuracy), and continuous-variable representations of crown closure (accuracies in the 90 percent range for a two-class configuration; 50 percent for four classes), and tree species composition (90 percent accuracy in a two-class configuration; 73 percent for four classes) (Figure 6). The layers were derived primarily from Landsat imagery, and represent 2003 ground conditions.

Data Sources

The study area is covered by Landsat path/row 44/23 and 45/23, and we acquired annual summer imagery from each scene from 1998 to 2005 to aid in our characterization changing forest conditions across this time interval (Table 1). The images were a blend of Landsat-5 Thematic Mapper (TM) and Landsat-7 Enhanced Thematic Mapper Plus (ETM+), and included a single ETM+ SLC-off scene (gap-filled) from 2004.

In addition to satellite data, we also acquired a variety of supplementary GIS data sets to aid in image processing and disturbance classification procedures. The Alberta government's 30-meter digital elevation model was used for orthorectification, and to derive additional slope and aspect layers used in the categorization of change. We also had access to the provincial road layer and a forest fire database, as well as agriculture and settlement masks developed by Collingwood (2007). The masks were used to exclude changes occurring within these two land-use zones, which occur primarily along the study area's eastern boundary.

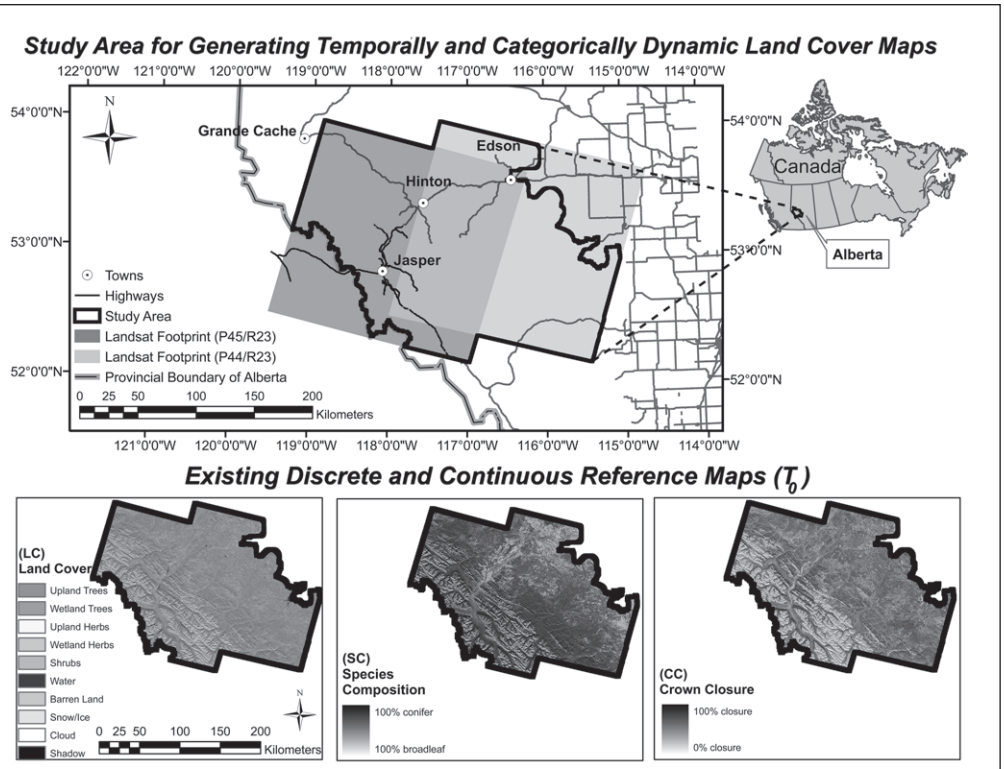

Figure 6. Location of the study area for generating temporally and categorically dynamic forest land-cover maps, where reference maps of discrete thematic land-cover and of continuous forest-cover attributes (species composition and crown closure) exist.

Pre-existing disturbances ($T_{\leq -5}$), for cutblocks were available from industrial forest landholders as digitized feature polygons. We also acquired as much orthophotography as possible, in order to facilitate the independent validation of change features. However, the availability of spatially coincident, consecutive, cloud-free orthophotography was limited to the years 2000 and 2001. Image processing procedures were performed in PCI Geomatica® 9.1, while segmentation and object-based classifications were performed using Definiens Professional 5.0. All vector and raster database management took place in ArcGIS® 9.2.

Implementation of the Framework

Generating the Disturbance Inventory

In characterizing changes on the landscape, we focused our efforts on the six types of forest-replacing disturbances

Table 1. Remote Sensing Imagery used for the Detection of Disturbance Features with Time Assignments in Reference to the Methodological Framework for Generating the Disturbance Inventory

Landsat Path/Row	Image Acquisition Date	Sensor	Time Assignment acc. to Disturbance Inventory Framework
45/23	05 September 1998	Landsat-5 TM	T_{-5}
	08 September 1999	Landsat-5 TM	T_{-4}
	17 August 2000	Landsat-7 ETM+	T_{-3}
	14 September 2001	Landsat-7 ETM+	T_{-2}
	23 August 2002	Landsat-7 ETM+	T_{-1}
	03 September 2003	Landsat-5 TM	T_0
	12 August 2004	Landsat-7 SLC-Off	T_{+1}
	22 July 2005*	Landsat-5 TM	T_{+2}
44/23	29 August 1998	Landsat-7 ETM+	T_{-5}
	24 August 1999*	Landsat-7 ETM+	T_{-4}
	27 September 2000*	Landsat-7 ETM+	T_{-3}
	14 September 2001	Landsat-7 ETM+	T_{-2}
	13 June 2002	Landsat-7 ETM+	T_{-1}
	10 July 2003*	Landsat-5 TM	T_0
	13 August 2004	Landsat-5 TM	T_{+1}
	13 September 2005	Landsat-5 TM	T_{+2}

*indicates >10% Clouds

that dominate the study area: (a) *burns* from forest fires, (b) *cutblocks* from forest clearcutting, (c) *mines* from surface extraction for coal and gravel, (d) *wellsites* from petroleum extraction, (e) *pipelines* from oil and gas transportation, and (f) *roads* from mechanized human access (Table 2). Because of the scale at which mapping activities took place, we treated burns, cutblocks, and mines as areal features, wellsites as point features, and roads and pipelines as linear features. These feature classes will be adhered to throughout this framework implementation, though applications in other landscapes (or using other remote sensing data sets) might assign features differently. In following the nomenclature introduced in the manuscript previously, we will refer to the 2003 reference year as T_0, while 1998 is T_{-5}, and 2005 is T_{+2}.

An overview of the entire methodological flowchart used to generate the inventory of disturbance features outlined above is summarized in Figure 7. The procedure is comprised of 19 steps, organized into three major components: (Part A) annual disturbance mapping, (Part B) pre-existing disturbance mapping, and (Part C) disturbance inventory conditioning. Each part is described briefly below, with the steps corresponding to those listed in Figure 7.

Annual Disturbance Mapping (Part A)

All TM and ETM+ images were converted to at-satellite reflectance following the methods of Chander and Markham (2003) to improve the radiometric consistency between scenes and sensor types. Each image was then orthorectified to a root mean square error tolerance of 0.5 pixels, and re-sampled using nearest-neighbor to 30-meter pixels in UTM Zone 11, NAD83, based on the GRS80 ellipsoid. The result of this preprocessing was a spatially accurate, radiometrically consistent time series of Landsat images representing T_{-5} to T_{+2} ground conditions (Figure 7, Step 1). We used the enhanced wetness difference index (EWDI) method of Franklin *et al.* (2001) to generate *difference* layers designed to characterize the changes observed along each step in the temporal time sequence (Figure 7, Step 2). EWDI has been shown to be an effective strategy for forest disturbances, and the technique has been successfully employed under a variety of conditions in previous studies (e.g., Franklin *et al.*, 2002; Skakun *et al.*, 2003). The annual difference layers were segmented in Definiens 5.0, using parameters of 10 for scale, 0.1 for shape, and 0.7 for compactness. The resulting vector layers were manually thresholded using the mean EWDI value into *change* and *no change* objects using visual inspection of the respective image pairs (Figure 7, Step 3). The *change* objects became the basis for all subsequent disturbance mapping for areal features.

With a decision tree approach, *change* objects were classified into areal disturbance categories (cutblocks, mines, and burns), using attributes related to the object's spectral characteristics, size, shape, and context (Figure 7, Step 4). In order to minimize errors in the annual disturbance mapping, the results of the areal disturbance classification were visually inspected and corrected where necessary. Linear and point features, although visually detectable from the imagery, could not be reliably mapped using automated detection and classification methods, since the resolution of the imagery was not sufficient to yield consistent and discrete object delineations for these features. As a result, change objects related to these feature types were discarded.

We used manual digitizing to delineate point and linear disturbance features associated with wellsites, roads, and pipelines with reference to the available imagery (Figure 7, Steps 5 and 6). Wellsites were characterized with 3×3 pixel squares centered around each new wellsite location, with the boundaries snapped to the grid of the reference land-cover map (LC T_0). The centerlines of linear features were digitized as polylines and converted to polygon features using a total buffer width of 60 meters (i.e., 2 pixels). Linear features were visually classified into roads and pipeline on the basis of surface vegetation characteristics. Once again, the resulting features were rasterized and snapped to the T_0 reference map in order to create consistent boundary delineations, in preparation for seamless integration with other disturbance features and map products. Next, all the annual disturbance features (areal, linear, and point) were merged into an annual disturbance database, including attribute information that specified disturbance type and year of origin (Figure 7, Step 7).

Pre-existing Disturbance Mapping (Part B)

In order to incorporate areal disturbance features existing on the landscape prior to 1998 (T_{-5}) into the disturbance inventory, we selected digitized polygons representing cutblocks, mines, and burns from ancillary GIS sources on the basis of attributes. In order to ensure seamless integration of these entities with the other map products, we used overlay procedures to extract the corresponding polygons of pre-existing features as depicted in the T_0 reference map (Figure 7, Step 8). This spatial overlay operation yielded a multitude of potential pre-disturbance features, which needed to be attributed according to land-cover characteristics.

TABLE 2. FEATURE TYPE, DISTURBANCE TYPE, SPATIAL OVERLAY ORDER (INCREASING NUMBERING CORRESPONDS TO BOTTOM-UP DIRECTION), AND LAND-COVER TRANSITION RULES FOR DISTURBANCE FEATURES MAPPED IN THE STUDY AREA ($T_{<D}$ refers to the Points in Time Prior to the Origination of the Disturbance Feature, T_D refers to the Point in Time when the Disturbance Originated, and T_{D+n} refers to the Point in Time after a Disturbance Feature Originated as Specified by the Time Interval *n*, in this Case, Years)

			Land-cover (LC) Transition Rules			
	Disturbance Features		Pre-disturbance LC label for *backdating*	Post-disturbance LC label for *backdating and updating*		
Feature Type	Disturbance Type	Overlay Order	$T_{<D}$	T_D	$T_{D+1} - T_{D+2}$	$T_{>D+2}$
Area	Burn	1	Forest	Barren	Herb	Shrub
Area	Cutblock	2	Forest	Barren	Herb	Shrub
Area	Mine	3	Forest	Barren	Barren	Barren
Linear	Pipeline	4	no data	Herb	Herb	Herb
Linear	Road	5	no data	Barren	Barren	Barren
Point	Wellsite	6	context determined	Barren	Barren	Barren

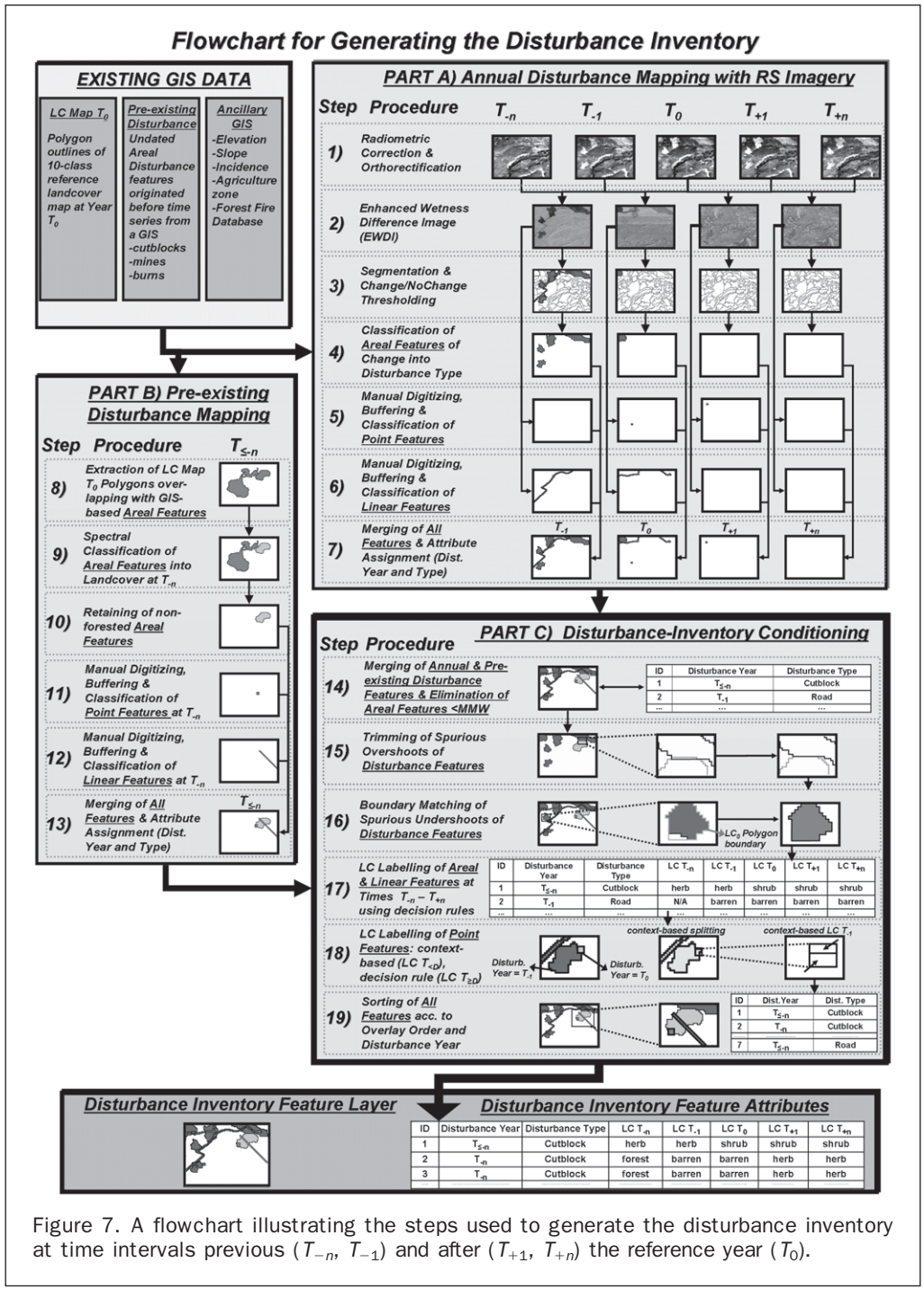

Figure 7. A flowchart illustrating the steps used to generate the disturbance inventory at time intervals previous (T_{-n}, T_{-1}) and after (T_{+1}, T_{+n}) the reference year (T_0).

The pool of potential pre-disturbance features included entities which had already transitioned to mature forest at the beginning of our time series (T_{-5}), and therefore no longer constituted dynamic features capable of displaying successional change over the investigated time frame. These features had to be removed. Since no land-cover or temporal attribute information existed in the ancillary disturbance database, we performed a supervised classification using 1998 Landsat imagery to identify pre-existing land-cover values. Each entity was classified as either barren, herbaceous, shrub, or other (unclassified) (Figure 7, Step 9). We then removed all the unclassified disturbance features from the disturbance inventory so that the resulting set of pre-disturbance features corresponded only to dynamic features (Figure 7, Step 10). All the point and linear features that were visually discernable on the multi-spectral imagery at the beginning of the time series (T_{-5}) were manually digitized and converted using the same procedures as described in Steps 5 and 6 (Figure 7, Steps 11 and 12). We then merged all the pre-existing disturbance features into a database, including attributes for date, year, and disturbance type (Figure 7, Step 13).

Disturbance-Inventory Conditioning (Part C)

The databases for annual and pre-existing disturbance features were merged to create a single disturbance inventory

database containing all dynamic features on the landscape over the time frame of this study (T_{-5} to T_{+2}) (Figure 7, Step 14). Despite our efforts to limit image registration errors, the disturbance features exhibited spurious overshoots and undershoots with the boundaries of coinciding and adjacent reference features, as well as with other adjacent disturbance features (this issue was described previously, and illustrated in Figure 4). We used visual comparison of the relative positioning of mapped features with the respective Landsat images to determine the minimum mapping width (MMW) requirement for real changes manifesting themselves in updated and backdated maps. The observed maximum deviation for spurious mismatches was just below 120 m for coinciding features and 60 m for adjacent features, corresponding to MMW's of four and two pixels respectively. In order to eliminate spurious change caused by misregistration, all areal disturbance that fell below the respective MMW's were discarded, hereby treating the features originating before 2003 (i.e., the disturbance year $T_{<0}$) as "coinciding features" and all others as "adjacent features." Point and linear features were excluded from this rule, since they were manually digitized and verified.

The remaining steps in Part C relate to the processing and management of the final disturbance inventory, in order to conform to the principles necessary for seamlessly integrating the disturbance features into the reference map. First, the trimming of spurious overshoots was handled (Figure 7, Step 15), beginning with adjacent disturbance features. Since it was feasible for *point* and *linear* features in the disturbance inventory (e.g., wellsites, roads, and pipelines) to overlap other disturbance features on the ground over time, no boundary trimming procedures were applied to these features. However, in order to account for spurious overshoots between adjacent *areal* features of the same disturbance type (cutblocks, mines, and burns could overlap other features on the ground, but not with features of their own type), we employed a bottom-up temporal approach to erase overlaps. Features originating in later years were trimmed or erased using the boundaries of disturbance features originating in earlier years. Spurious overshoots with boundaries of coinciding features in the reference map were corrected by creating an intersection between all disturbance features originating before 2003 (i.e., disturbance year $T_{<0}$) and all reference-map features (LC Map T_0 in Figure 7), and erasing the intersect portions that were contained within the MMW buffer around the boundaries of the selected disturbance features. We also applied a boundary-matching procedure to correct spurious boundary undershoots (Figure 7, Step 16), by identifying the *mismatch areas* between these undershoots, and then merging them with the nearest disturbance feature. In essence, we expanded the disturbance features to match the relevant reference boundaries (Figure 7, Step 16; see Linke *et al.*, 2009 for details).

Upon completion of the boundary-matching processing, the trimmed and expanded disturbance features were assigned land-cover labels for each of the backdated and updated years (Figure 7, Step 17), using simple decision rules (Table 2). *Cutblocks* and *burns* features were assigned to the "barren" class for the year in which they originated (T_D), "herbaceous" in the year following disturbance (T_{D+1}), and "shrub" in years two and beyond ($T_{\geq D+2}$). We did not allow disturbance features to progress beyond the shrub class, since the time frame of the study was considered shorter than the time horizon necessary for a mature forest stand to regenerate. *Road* and *mine* features were labeled as "barren" for all years, and *pipelines* were labeled "herbaceous." The land-cover labels for the years prior to the disturbance ($T_{<D}$) was assigned as 'forest" for all areal disturbance feature, under the assumption that all such disturbances were stand-replacing. The respective label for *roads* and *pipelines* was "no data" (an act that simply prevented their insertion in previous years), since they were not mapped in the 2003 reference land-cover map. All features that originated *after* the reference year ($T_{>0}$) were assigned "no data" labels for their pre-disturbance years.

The classification of post-disturbance land-cover for point features (Figure 7, Step 18) followed the same decision rules as those outlined above, but we used contextual information to assign pre-disturbance ($T_{\leq 0}$) land-cover labels (Table 2). While point features originating *after* the reference year ($T_{>0}$) were assigned "no data" labels for pre-disturbance years, many of the point features originating *prior* to T_0 were already mapped in the reference products, and therefore required the assignment of proper pre-disturbance land-cover categories. Unfortunately, we could not simply assume that all wellsites were cut from forests (like cutblocks), since they were commonly observed to occur on a variety of land-cover types. We therefore assigned pre-disturbance land-cover attributes for these features on the basis of context. Two separate situations were identified when extracting context for a wellsite: (a) the feature could be fully contained within a reference or disturbance feature, or (b) the feature could straddle two or more reference or disturbance features. In both cases, we used a 60-meter buffer (two Landsat pixel widths) to establish context. Wellsites occurring in the first situation were retained as whole entities, and assigned the land-cover class of the surrounding feature. Wellsites occurring in the second situation were split, with each entity receiving different land-cover classes (for an example of this, see ID #4a and ID #4b in Figure 2).

In the final step of disturbance inventory conditioning, the database was sorted according to spatial overlay order and disturbance year (Figure 7, Step 19; Table 2). Burns were arranged as the bottom layer (order 1), since cutblocks (order 2) (if spatially co-existing) could potentially overlap these features. Mines in our study area normally appeared on forested land, but nevertheless had the potential of overlapping with a cutblock or burn, and therefore were assigned the overlay order 3. Pipelines and roads could cross any disturbance feature, and were therefore assigned overlay orders 4 and 5, respectively. Wellsites occupied the top order, since these features were smaller than any other disturbance type and remained persistent throughout the time period.

Accuracy Assessment of the Disturbance Inventory

The disturbance inventory was tested for thematic accuracy across three phases of compilation: (a) change detectability, or the ability of the algorithm to discern *change* areas from *no change*, (b) disturbance type classification, or the ability to discriminate between cutblocks, wellsites, mines, burns, roads and pipelines, and (c) land-cover classification, or the accuracy of land-cover labels assigned to the disturbance features. The size of the assessment samples varied, depending on the accuracy assessment being performed. The sample size for change detectibility was obtained using methodology described by Husch *et al.* (2004), with the number of samples calculated as a function of the coefficient of variation in the pixel values and a 10 percent allowable error. As a result, we distributed 178 random samples proportionally between the *change* and *no-change* features: 5 and 173 samples, respectively. Since the classification of disturbance type produced nominal classes with no measurable variance, we calculated sample size for the second assessment using the method outlined in McCoy (2005) to arrive at a number of 256 with an allowable error of 20 percent. Those samples were randomly distributed proportionally to the area covered by each disturbance type. The same number of samples (256)

was randomly distributed for the nominal disturbance land-cover classification; again with size-proportional representation. User's, producer's, overall accuracies, and the kappa coefficient (Congalton and Green, 1999) were calculated for each of the three assessments.

Backdating and Updating of Reference Maps

Using the framework proposed in this paper, the discrete land-cover map of the study area (LC Map T_0 in Figure 6) was backdated and updated through the systematic overlay of features from the conditioned disturbance inventory (Figure 2 and Figure 5). The continuous reference maps (CC and SC Maps T_0 in Figure 6) were backdated through the overlay of crown closure and species composition models created with spectral variables derived from Landsat images from the first year of the time series (T_{-5}) using a mask area delineated by the conditioned disturbance features originating before T_0 (Figures 4 and 5). We used regression modeling to estimate crown closure and species composition from the reference maps (T_0) to spectral and topographic explanatory variables at T_{-5}. Sample data was collected randomly from the imagery in forested areas that were never disturbed throughout the entire time series. The approach is analogous to the model extension technique described by McDermid (2005), though the application here is temporal rather than spatial. In order to account for misregistration errors between the disturbance features and the continuous reference maps, the mask was buffered by two pixels. In the updating direction, areas corresponding to new disturbance features ($T_{D>0}$) were replaced with values of "0" for crown closure, and were assigned "no data" for species composition, since these areas were no longer considered forested.

Generating Temporally and Categorically Dynamic Land-cover Maps

The Grizzly Bear Map-O-Matic (GBMOM) is an ArcObjects program created in ArcGIS® 9.2, and is designed to generate a series of multi-temporal land-cover maps for any configuration of land-cover, species composition, and canopy closure through integrative post-processing. The program adds an important dynamic element to discrete land-cover products by allowing for user-specified class breaks, or categories, within the forest class. For demonstration purposes, we used the GBMOM to generate a series of categorically refined sample composite maps across the full eight-year time series. Upland forested areas were divided into five discrete land-cover categories: (a) Open Conifer (species composition: 80 to 100 percent coniferous, crown closure: 0 to 50 percent), (b) Moderate Conifer (species composition: 80 to 100 percent coniferous; crown closure: 51 to 70 percent), (c) Closed Conifer (species composition: 80 to 100 percent coniferous; crown closure: 71 to 100 percent), (d) Mixed Forest (species composition: 21 to 80 percent coniferous; crown closure 0 to 100 percent), and (e) Broadleaf Forest (species composition: 0 to 20 percent coniferous; crown closure 0 to 100 percent).

Results and Discussion

As previously described, the successful implementation of the proposed mapping framework depends on (a) the accurate detection and classification of disturbance features, and (b) the seamless integration of disturbance features into the existing reference maps. We have organized this section around each of these two components, followed by comments and observations related to the categorically refined nature of the resulting composite time series, and considerations about the general applicability of the framework.

Accurate Detection of Disturbance Features

We assessed the detection and classification of the disturbance inventory on the basis of three elements: (a) detection of change features, (b) classification of disturbance types, and (c) classification of land-cover. The results of all three assessments are summarized in Table 3.

The detection of change features produced excellent results, with an overall accuracy of 100 percent and a Kappa coefficient of 1.0. The EWDI change-detection procedure performed very well, and provided an effective tool for identifying change features in the study area. The classification of disturbance type had an overall accuracy of 98 percent and a "very good" Kappa agreement of 0.97. There was some minor confusion between disturbances features that appeared similar in the imagery. For example, some large wellsites and small burns were committed to the cutblock class. Among the manually digitized features, classification was perfect (Table 3).

The classification of land-cover for the disturbance features had an overall accuracy of 80 percent and a "good" Kappa agreement of 0.64. The decision rules used to assign land-cover labels to disturbance features in this implementation of the proposed framework was simplistic, relying only on idealized succession sequences (time from disturbance) and other basic rules. While the transition

TABLE 3. SUMMARY STATISTICS OF CONFUSION-MATRICES FOR CLASSIFICATION OF (1) CHANGE, AND NO CHANGE, (2) DISTURBANCE TYPE, AND (3) LAND-COVER

		Producer's Accuracy	User's Accuracy	Overall Accuracy	Kappa
	Change/No Change				
(1) Change Detection	Change	100%	100%		
	No Change	100%	100%	100%	1.0
	Disturbance Type				
(2) Disturbance Classification	Cutblock	100%	98%		
	Wellsite	92%	100%		
	Burn	85%	100%	98%	0.969
	Mine	100%	100%		
	Road	100%	100%		
	Pipeline	100%	100%		
	Land Cover Label				
(3) Land-cover Classification	Barren	56%	82%		
	Herb	74%	50%	80%	0.640
	Shrub	93%	89%		

rules succeeded in avoiding temporal inconsistencies, the actual rates of land-cover transition change varied from feature to feature, according to other influencing factors such as solar radiation, moisture, and soil type, which alter the rate of succession. The process could be refined through the use of spectral information from the imagery.

Seamless Integration of Disturbance Features

The trimming and expansion of spurious boundary-delineation mismatches, and the consistent application of spatial overlay order for features in the disturbance inventory were the factors most strongly influencing the seamless integration of disturbance features. Through careful implementation of the disturbance-inventory framework presented in this paper, we were successful in our attempts to produce spatially consistent maps of land-cover, crown closure, and species composition (Plate 1). We observed no spurious changes in the land-cover maps. For example, within a 5.4 km $\times$ 5.4 km sample area, several disturbances occurred in the form of new cutblocks (years 2000 to 2003, and 2005), new roads (years 2000 and 2005), and a wellsite (2000) (Plate 1). For the disturbance features that originated in 2003 or earlier, mismatched boundaries between the disturbance features and other adjacent features would have manifested themselves as small sliver objects or spurious gaps, especially conspicuous in the years before the disturbance appeared, had they not been suppressed (McDermid *et al.*, 2008). The absence of these errors emphasizes the importance of boundary matching, and the success of the methods implemented here. Furthermore, as demonstrated in this sample, the spatial overlay order ensured that linear features remained visible when they occurred in conjunction with an areal feature. When several cutblocks transitioned to herbaceous and shrub cover types in 2004 and 2005, roads features traversing these areas remained visible.

In the continuous maps of crown closure and species composition, the integration of the regression model (applied to the Landsat TM imagery at year T_{-5} (1998) within the buffered area of the disturbance inventory) yielded seamless map products without spurious values. In Plate 1, we can see areas corresponding to cutblocks originating between 2000 and 2003 that blend seamlessly in the years prior to their appearance.

Temporally and Categorically Dynamic Map Composite

By successfully creating a spatially consistent time series that blends categorical characterization of basic land-cover with continuous-variable representations of crown closure and species composition, the disturbance-inventory framework implemented here enables the production of temporally and categorically dynamic forest land-cover maps (Figure 5). The composite map generated in this implementation with the GBMOM exemplifies one of such possible case, and reveals the value of the proposed approach (Plate 1).

Considerations Regarding the General Applicability of the Framework

For the first time, a framework has been described that enables the generation of land-cover maps, which are dynamic in their categorical definition and therefore capable of adapting to support a variety of applications. Since these maps are also updated by automated remote-sensing methods to yield products that are spatially consistent across time, we consider them an appropriate basis for conducting efficient and reliable landscape monitoring. The disturbance inventory is open to features delineated by different processing methods (manual digitizing, automatic segmentation)

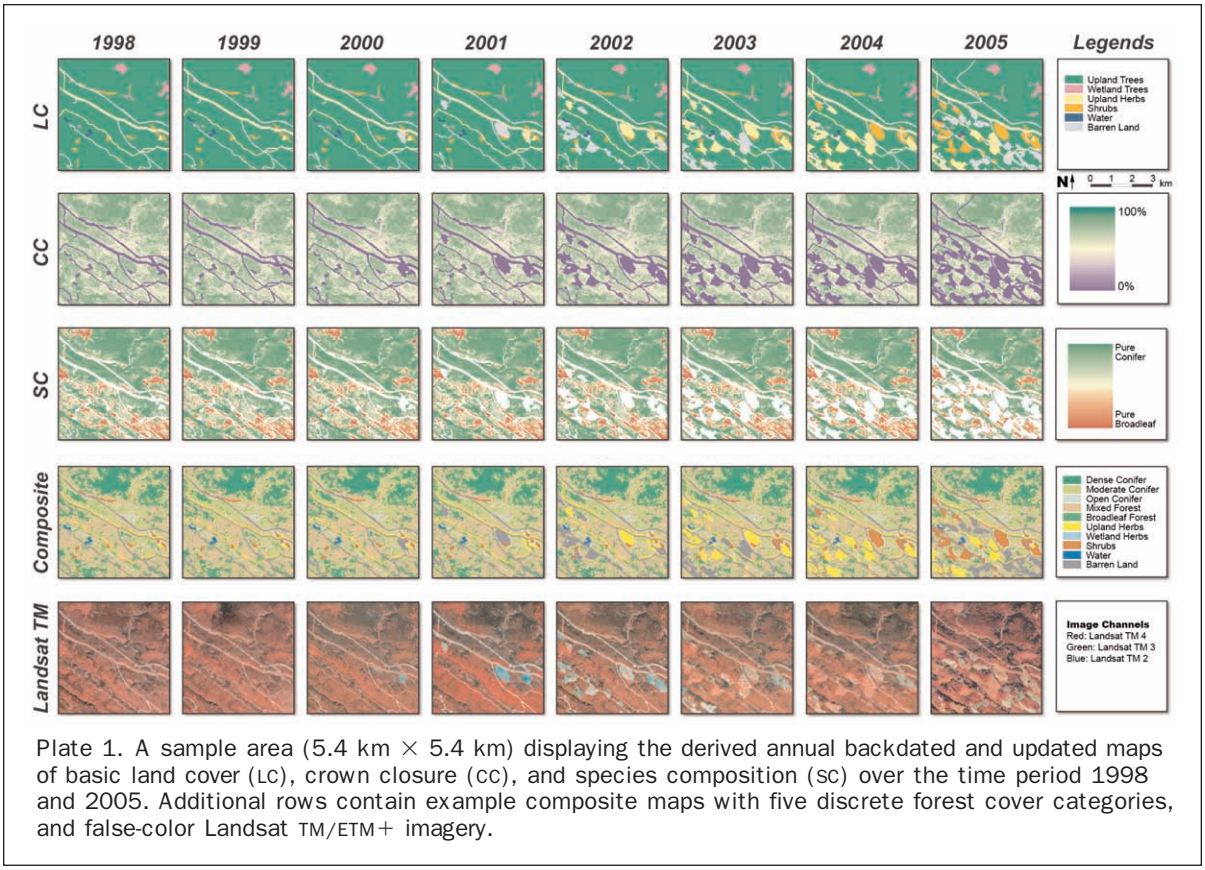

Plate 1. A sample area (5.4 km $\times$ 5.4 km) displaying the derived annual backdated and updated maps of basic land cover (LC), crown closure (CC), and species composition (SC) over the time period 1998 and 2005. Additional rows contain example composite maps with five discrete forest cover categories, and false-color Landsat TM/ETM+ imagery.

from different image sources (Landsat in this case), as long as the boundary-matching conditions can still be adhered to. Further, the disturbance inventory is not limited to the initial time frame investigated, but can easily be appended when images from additional years become available.

While our experience here demonstrates the effectiveness of the overall approach, the results are still subject to errors in the T_0 reference map. Since the proposed framework does not alter the reference map outside disturbance features, errors present in the *no change* areas will persist throughout the time series. However, these errors remain consistent, and with the focus on reliable landscape monitoring, are much less troubling than the stochastic spatial errors dealt with in our approach. Linke *et al.* (2009) showed that boundary-delineation errors arising from the mismatched integration of change features had a large impact on landscape metrics, and led to significant distortions in landscape pattern analysis. These errors were successfully suppressed in this work by matching the boundaries of change features, both to each other and to corresponding objects in the reference maps.

In addition to the internal dynamics of specific disturbance features, the size and shape of a ground feature may also change through time. Within the context of our framework, these modifications constitute discrete disturbance events which are spatially adjacent to, or contained by, the ground feature in question. As a result, these occurrences are dynamic features themselves. For example, the *increase* (e.g., a fire-driven expansion of a barren cutblock area through the burning of an adjacent forest section) or *decrease* (e.g., the advanced forest succession of a fenced section in a cutblock to reduce deer-browsing) in area of a ground feature with time can be represented by means of *feature insertions* and *feature removals*, as overlaid in context to adjacent dynamic features. However, it should be noted that the MMW requirements for the detection of areal dynamic features (Step 14, Figure 7) prevents any representations of feature increases or decreases below these minimum specifications.

Conclusions

A framework for generating temporally and categorically dynamic forest land-cover maps has been presented. The work constitutes an innovative approach designed to enable the seamless updating and backdating of existing map products based on a combination of different types of disturbance features, delineated by manual or automatic methods, stored in a disturbance-inventory database and conditioned with boundary-matching procedures and overlay orders. By implementing the framework over an eight-year time interval across a large, multi-use study area in western Alberta, we demonstrated that the resulting products are reliable, and free of artifacts generated through the mismatched integration of change features. Furthermore, by accommodating both categorical and continuous-variable maps, the approach allows for flexible monitoring at any categorical scale of interest: an important consideration for specific wildlife and environmental applications. While our framework does not eliminate pre-existing errors in the reference maps, it successfully enables the production of reliable, spatially consistent representations of landscape dynamics through time by suppressing the introduction of new errors.

Acknowledgments

This work has been funded in part through the Natural Science and Engineering Research Council of Canada. Julia Linke was directly supported by a NSERC PGS B scholarship and an Alberta Ingenuity Award. We gratefully acknowledge the support of Foothills Research Institute Grizzly Bear Research Program and its many partners in government, academics, and industry. We also extend thanks to Guillermo Castilla for many helpful communications during the development of this research, and to two anonymous reviewers who (along with Dr. B. Huang) provided constructive comments on an earlier version of this manuscript.

References

Berland, A., T. Nelson, G. Stenhouse, K. Graham, and J. Cranston, 2008. The impact of landscape disturbance on grizzly bear habitat use in the Foothills Model Forest, Alberta, Canada, *Forest Ecology and Management*, 256:1875–1883.

Betts, M.G., G.J. Forbes, and A.W. Diamond, 2007. Thresholds in songbird occurrence in relation to landscape structure, *Conservation Biology*, 21:1046–1058.

Blaschke, T., 2005. Towards a framework for change detection based on image objects, *Göttinger Geographische Abhandlungen* (S. Erasmi, B. Cyffka, and M. Kappas, editors), 113:1–9.

Boentje, J.P., and M.S. Blinnikov, 2007. Post-Soviet forest fragmentation and loss in the Green Belt around Moscow, Russia (1991-2001): A remote sensing perspective, *Landscape and Urban Planning*, 82:208–221.

Brown, D.G., J.-D. Duh, and S.A. Drzyzga, 2000. Estimating error in an analysis of forest fragmentation change using North American Landscape Characterization (NALC) data, *Remote Sensing of Environment*, 71:106–117.

Chander, G., and B. Markham, 2003. Revised Landsat-5 TM radiometric calibration procedures and postcalibration dynamic ranges, *IEEE Transactions on Geoscience and Remote Sensing* 41(11):2674–2677.

Chrisman, N.R., 1989. Modelling error in overlaid maps, *Accuracy of Spatial Databases* (M.F. Goodchild and S. Goopal, editors), CRC Press, London, pp. 21–34.

Congalton, R.G., and K. Green, 1999. Assessing the Accuracy of Remotely Sensed Data: Principles and Practices, Lewis Publishers, Boca Raton, Florida, 137 p.

Collingwood, A., 2007. *Satellite Image Classification and Spatial Analysis of Agricultural Areas for Land Cover Mapping of Grizzly Bear Habitat*, M.Sc. thesis, University of Saskatchewan, Saskatoon, Saskatchewan, 127 p.

Conard, S.G., A.I. Sukhinin, B.J. Stocks, D.R. Cahoon, E.P. Davidenko, and G.A. Ivanova, 2002. Determining effects of area burned and fire severity on carbon cycling and emissions in Siberia, *Climatic Change*, 55:197–211.

Coppin, P.R., and M.E. Bauer, 1996. Digital change detection in forest ecosystems with remote sensing imagery, *Remote Sensing Reviews*, 13:207–234.

Coppin, P.R., I. Jonckheere, K. Nackaerts, B. Muys, and E. Lambin, 2004. Digital change detection methods in ecosystem monitoring: A review, *International Journal of Remote Sensing*, 25:1565–1596.

Desclée, B., P. Bogaert, and P. Defourny, 2006. Forest change detection by statistical object-based method, *Remote Sensing of Environment*, 102:1–11.

Feranec, J., G. Hazeu, S. Christensen, and G. Jaffrain, 2007. Corine land cover change detection in Europe (case studies of the Netherlands and Slovakia), *Land Use Policy*, 24:234–247.

Feranec, J., M. Suri, J. Otahel, T. Cebecauer, J. Kolar, T. Soukup, D. Zdenkova, J. Waszmuth, V. Vajdea, A. Vijdea, and C. Nitica, 2000. Inventory of major landscape changes in the Czech Republic, Hungary, Romania and Slovak Republic, *International Journal of Applied Earth Observation and Geoinformation*, 2:129–139.

Forrest, J.L., E.W. Sanderson, R. Wallace, T.M.S. Lazzo, L.H.G. Cervero, and P. Coppolillo, 2008. Patterns of land cover change in and around Madidi National Park, Bolivia, *Biotropica*, 40:285–294.

Franklin, S.E., M.B. Lavigne, L.M. Moskal, and T.M. McCaffrey, 2001. Interpretation of forest harvest conditions in New Brunswick using Landsat TM enhanced wetness difference imagery (EWDI), *Canadian Journal of Remote Sensing*, 27(1):118–128.

Franklin, S.E., M.B. Lavigne, M.B. Wulder, and T.M. McCaffrey, 2002. Large-area forest structure change detection: An example, *Canadian Journal of Remote Sensing*, 28(14):588–592.

Franklin, S.E., 2001. *Remote Sensing for Sustainable Forest Management*, Lewis Publishers, Boca Raton, Florida, 407 p.

Gamanya, R., P. De Maeyer, and M. De Dapper, 2009. Object-oriented change detection for the city of Harare, Zimbabwe, *Expert Systems with Applications*, 36(1):571–588.

Goodchild, M.F., 1978. Statistical aspects of the polygon overlay problem, *Harvard Papers on Geographic Information Systems (Volume 6)* (G. Dutton, editor), Addison-Wesley, Reading, Massachusetts, pp. 1–22.

Gottschalk, T., and F. Huettmann, 2006. Thirty years of analyzing and modeling avian habitat relationships using satellite imagery data: A review, *Journal of Ornithology*, 147:175–175.

Hansen, A.J., R.P. Neilson, V.H. Dale, C.H. Flather, L.R. Iverson, D.J. Currie, S. Shafer, R. Cook, and P.J. Bartlein, 2001. Global change in forests: Responses of species, communities, and biomes, *Bioscience*, 51(9):765–779.

Homer, C, J. Dewitz, J. Fry, M. Coan, N. Hossain, C. Larson, N. Herold, A. McKerrow, J.N. VanDriel, and J. Wickham, 2007. Completion of the 2001 National Land Cover Database for the conterminous United States, *Photogrammetric Engineering & Remote Sensing*, 73(4):337–341.

Houghton, R.A., 1994. The worldwide extent of land-use change, *Bioscience*, 44:305–313.

Houghton, R.A., Y. Ding, D.J. Griggs, M. Noguer, P.J. van der Linden, X. Dai, K. Maskell, and C.A. Johnson (editors), 2001. Climate Change 2001: *The Scientific Basis. Contribution of Working Group I to the Third Assessment Report of the Intergovernmental Panel of Climate Change*, Cambridge University Press, Cambridge, UK, 881 p.

Huang, C., S. Kim, A. Altstatt, J.R.G. Townshend, P. Davis, K. Song, C.J. Tucker, O. Rodas, A. Yanosky, R. Clay, and J. Musinsky, 2007. Rapid loss of Paraguay's Atlantic forest and the status of protected areas - A Landsat assessment, *Remote Sensing of Environment*, 106(4):460–466.

Husch, B., J.A. Kershaw, and T.W. Beers, 2003. *Forest Mensuration*, Fourth edition), Wiley, New York, 319 p.

Jansen, L.J.M., M. Bagnoli, and M. Focacci, 2008. Analysis of land-cover/use change dynamics in Manica Province in Mozambique in a period of transition (1990–2004), *Forest Ecology and Management*, 254(2):308–326.

Jansen, L.J.M., G. Carrai, L. Morandini, P.O. Cerutti, and A. Spisni, 2006. Analysis of the spatio-temporal and semantic aspects of land-cover/use change dynamics 1991–2001 in Albania at national and district levels, *Environmental Monitoring and Assessment*, 119:107–136.

Käyhkö, N., and H. Skånes, 2006. Change trajectories and key biotopes - Assessing landscape dynamics and sustainability, *Landscape and Urban Planning*, 75:300–321.

Kozak, J., C. Estreguil, and P. Vogt, 2007. Forest cover and pattern changes in the Carpathians over the last decades, *European Journal of Forest Research*, 126:77–90.

Kuemmerle, T., P. Hostert, V.C. Radeloff, K. Perzanowski, and I. Kruhlov, 2007. Post-socialist forest disturbance in the Carpathians, *Ecological Applications*, 17(5):1279–1295.

Langford, W.T., S.E. Geregel, T.G. Dietterich, and W. Cohen, 2006. Map misclassification can cause large errors in landscape pattern indices: Examples from habitat fragmentation, *Ecosystems*, 9:474–488.

Linke, J., G.J. McDermid, A. Pape, A.J. McLane, D.N. Laskin, M. Hall-Beyer, and S.E. Franklin, 2009. The influence of patch-delineation mismatches on multi-temporal landscape pattern analysis, *Landscape Ecology*, 24(2):157–170.

Linke, J., S.E. Franklin, F. Huettmann, and G. Stenhouse, 2005. Seismic cutlines, changing landscape metrics and grizzly bear landscape use in Alberta, *Landscape Ecology*, 20(7):811–826.

Lu, D., P. Mausel, E. Brondizio, and E. Moran, 2004. Change detection techniques, *International Journal of Remote Sensing*, 25:2365–2407.

Mas, J., 2005. Change estimates by map comparison: A method to reduce erroneous changes due to positional error, *Transactions in GIS*, 9:619–629.

McCoy, R.M., 2005. *Field Methods in Remote Sensing*, Guilford Press, New York, 159 p.

McDermid, G.J., 2005. *Remote Sensing for Large-Area, Multi-Jurisdictional Habitat Mapping*, Ph.D. Thesis, University of Waterloo, Waterloo, Ontario, 258 p.

McDermid, G.J., S.E. Franklin, and E.F. LeDrew, 2005. Remote sensing for large-area habitat mapping, *Progress in Physical Geography*, 29(4):449–474.

McDermid, G.J., A.D. Pape, J. Linke, D.N. Laskin, A.J. McLane, and S.E. Franklin, 2008. Object-based approaches to change detection and thematic map update: Challenges and limitations, *Canadian Journal of Remote Sensing*, 34(5):462–466.

McGarigal, K., and S. Cushman, 2005. The gradient concept of landscape structure, *Issues and Perspectives in Landscape Ecology* (J. Wiens and M. Moss, editors), Cambridge University Press, Cambridge, UK, pp. 112–119.

Nielsen, S.E., M.S. Boyce, and G.B. Stenhouse, 2004. Grizzly bears and forestry, I.: Selection of clearcuts by grizzly bears in west-central Alberta, Canada, *Forest Ecology and Management*, 199:51–65.

Nielsen, S.E., M.S. Boyce, G.B. Stenhouse, and R.H.M. Munro, 2002. Modeling grizzly bear habitats in the Yellowhead Ecosystem of Alberta: Taking autocorrelation seriously, *Ursus*, 13:153–164.

Pearson, S.M., M.G. Turner, and J.B. Drake, 1999. Landscape change and habitat availability in the Southern Appalachian Highlands and Olympic Peninsula, *Ecological Applications*, 9(4):1288–1304.

Plummer, S.E., 2000. Perspectives on combining ecological process models and remotely sensed data, *Ecological Modelling*, 129:169–186.

Radke, R.J., S. Andra, O. Al-Kofahi, and B. Roysam, 2005. Image change detection algorithms: A systematic survey, *IEEE Transactions on Image Processing*, (14):294–307.

Reyes, E., M.L. White, J.F. Martin, G.P. Kemp, J.W. Day, and V. Aravamuthan, 2000. Landscape modeling of coastal habitat change in the Mississippi delta, *Ecology*, 81:2331–2349.

Riitters, K.H., J.D. Wickham, R.V. O'Neill, K.B. Jones, E.R. Smith, J.W. Coulston, T.G. Wade, and J.H. Smith, 2002. Fragmentation of continental United States forests, *Ecosystems*, 5:815–822.

Rogan, J., and D. Chen, 2004. Remote sensing technology for mapping and monitoring land-cover and land-use change, *Progress and Planning*, 61(4):301–325.

Sader, S.A., and K.R. Legaard, 2008. Inclusion of forest harvest legacies, forest type, and regeneration spatial patterns in updated forest maps: A comparison of mapping results, *Forest Ecology and Management*, 255:3846–3856.

Shao, G., and J. Wu, 2008. On the accuracy of landscape pattern analysis using remote sensing data, *Landscape Ecology*, 23:505–511.

Skakun, R.S., M.B. Wulder, and S.E. Franklin, 2003. Sensitivity of the EWDI to mountain pine beetle red-attack damage, *Remote Sensing of Environment*, 86(4)433–443.

Skole, D.L., and C.J. Tucker, 1993. Tropical deforestation and habitat fragmentation in the Amazon: Satellite data from 1978 to 1988, *Science*, 260:1905–1910.

Song, C., T.A. Schroeder, and W.B. Cohen, 2007. Predicting temperate conifer forest successional stage distributions with multitemporal Landsat Thematic Mapper imagery, *Remote Sensing of Environment*, 106:228–237.

Stenhouse, G., and K. Graham, 2007. *Foothills Model Forest Grizzly Bear Research Program: 2006 Annual Report*, Foothills Model Forest, Hinton, Alberta, 67 p.

Thogmartin, W.E., A.L. Gallant, M.G. Knutson, T.J. Fox, and M.J. Suarez, 2004. Commentary: A cautionary tale regarding

use of the National Land Cover Dataset 1992, *Wildlife Society Bulletin*, 32:970–978.

Van Oort, P.A.J., 2005. Improving land cover change estimates by accounting for classification errors, *International Journal of Remote Sensing*, 26(14):3009–3024.

Vester, H.F.M., D. Lawrence, J.R. Eastman, B.L. Turner, S. Calme, R. Dickson, C. Pozo, and F. Sangermano, 2007. Land change in the southern Yucatan and Calakmul Biosphere Reserve: Effects on habitat and biodiversity, *Ecological Applications*, 17:989–1003.

Wiens, J.A., 1994. Habitat fragmentation: Island versus landscape perspectives on bird conservation, *Ibis*, 137(S1):S97–S104

Woodcock, C.E., A.A. Allen, M. Anderson, A.S. Belward, R. Bindschadler, W.B. Cohen, F. Gao, S.N. Goward, D. Helder, E. Helmer, R. Nemani, L. Oreapoulos, J. Schott, P.S. Thenkabail, E.F. Vermote, J. Vogelmann, M.A. Wulder, and R. Wynne, 2008. Free access to Landsat imagery, *Science*, 320:1011.

Yuan, D., and C. Elvidge, 1998. NALC land cover change detection pilot study: Washington D.C. area experiments, *Remote Sensing of Environment*, 66:166–178.